Geophysical Research Letters

RESEARCH LETTER
10.1029/2020GL090376

Wind Speed, Surface Flux, and Intraseasonal Convection Coupling From CYGNSS Data

Hien X. Bui[1], Eric D. Maloney[1], Emily M. Riley Dellaripa[1], and Bohar Singh[2]

[1]Department of Atmospheric Science, Colorado State University, Fort Collins, CO, USA, [2]International Research Institute for Climate and Society, Columbia University, New York, NY, USA

Abstract This study analyzes wind speed and surface latent heat flux anomalies from the Cyclone Global Navigation Satellite System (CYGNSS), aiming to understand the physical mechanisms regulating intraseasonal convection, particularly associated with the Madden-Julian oscillation (MJO). An advantage of CYGNSS compared to other space-based data sets is that its surface wind speed retrievals have reduced attenuation by precipitation, thus providing improved information about the importance of wind-induced surface fluxes for the maintenance of convection. Consistent with previous studies from buoys, CYGNSS shows that enhanced MJO precipitation is associated with enhanced wind speeds, and that associated surface heat flux anomalies have a magnitude about 7–12% of precipitation anomalies. Thus, latent heat flux anomalies are an important maintenance mechanism for MJO convection through the column moist static energy budget. A composite analysis during boreal summer over the eastern north Pacific also supports the idea that wind-induced surface flux is important for MJO maintenance there.

Plain Language Summary Enhanced surface evaporation (equivalent to a term called latent heat flux) during high wind speed periods can support precipitation through atmospheric moistening. Such evaporation anomalies form a key air-sea interaction component of the Madden-Julian oscillation (MJO). Based on the wind speed and related evaporation anomalies derived from Cyclone Global Navigation Satellite System (CYGNSS) measurements, we show that (1) enhanced MJO precipitation is associated with enhanced wind speed and surface evaporation that may help support the MJO in the Indo-Pacific warm pool and (2) enhanced local surface evaporation is important for maintenance of the MJO over the eastern north Pacific during Northern Hemisphere summer. These results verify results from previous buoy studies that suggest the importance of enhanced wind-driven surface evaporation for maintaining the MJO.

Key Points:
- CYGNSS wind speed and latent heat flux are used to quantify the feedback of wind-induced surface fluxes on MJO convection
- Enhanced MJO precipitation is associated with enhanced wind speed and latent heat anomalies that are about 7–12% of precipitation anomalies
- The wind-induced surface flux feedback is also important for MJO convection during the boreal summer in the eastern north Pacific

Supporting Information:
- Supporting Information S1

Correspondence to:
H. X. Bui,
hien.bui@colostate.edu

Citation:
Bui, H. X., Maloney, E. D., Riley Dellaripa, E. M., & Singh, B. (2020). Wind speed, surface flux, and intraseasonal convection coupling from CYGNSS data. *Geophysical Research Letters*, *47*, e2020GL090376. https://doi.org/10.1029/2020GL090376

Received 14 AUG 2020
Accepted 13 OCT 2020
Accepted article online 26 OCT 2020

1. Introduction

This study addresses the importance of wind-induced surface fluxes to the maintenance of the Madden-Julian oscillation (MJO; Madden & Julian, 1971, 1972), which is the dominant mode of tropical intraseasonal variability (Zhang, 2005, 2013). Over the tropical oceans, higher wind speeds are generally associated with larger surface heat fluxes and thus enhanced precipitation and convection (Back & Bretherton, 2005). On the intraseasonal timescale, MJO surface flux anomalies have been shown to be dominated by the wind-driven component (e.g., Araligidad & Maloney, 2008; Riley Dellaripa & Maloney, 2015; Shinoda et al., 1998). These wind-induced fluxes can affect the propagation, growth, and maintenance of the MJO (e.g., DeMott et al., 2015, and reference therein; Klingaman & Woolnough, 2014). For example, surface fluxes may help regulate the amplitude of MJO precipitation as several modeling studies showed weakened MJO amplitude when intraseasonal wind-surface flux feedbacks were removed (e.g., Maloney & Sobel, 2004; Maloney et al., 2010; Sobel et al., 2010; and many others). Hence, understanding the role of wind-induced surface flux is necessary for a comprehensive understanding of the dynamics of the MJO.

One impact of surface flux anomalies associated with the MJO is to modulate sea surface temperature (SST) that can feed back onto convection (e.g., DeMott et al., 2015). Zhang and McPhaden (2000) showed that intraseasonal variations of surface latent heat flux and shortwave radiation associated with intraseasonal disturbances can alter SST by up to 1°C. Such SST variations can help modulate intraseasonal convection (Maloney & Sobel, 2004). Another impact of surface flux anomalies to the MJO is through its direct impact on convection through the moist static energy (MSE) and moisture budgets—which will

be the focus of this study. Previous studies have shown that a buildup of moisture and MSE occurs before an MJO precipitation event that is dominated by horizontal advection and contributes to propagation, with maxima of MSE and precipitation nearly in phase (e.g., Andersen & Kuang, 2012; Maloney, 2009). Radiative heating anomalies and surface flux anomalies have been previously suggested to help maintain the MSE and precipitation anomaly (e.g., Adames & Kim, 2016; Wolding & Maloney, 2015). Riley Dellaripa and Maloney (2015) showed using Research Moored Array for African-Asian-Australian Monsoon Analysis and Prediction (RAMA) buoy data over the Indian ocean that intraseasonal latent heat flux anomalies are approximately 8% of intraseasonal precipitation anomalies, compared to about 17% from outgoing longwave radiation (OLR; Adames & Kim, 2016). This suggests the potential of wind-induced latent heat fluxes to aid maintenance of MJO convection when compared to the approximate 20% export due to column-integrated vertical MSE advection (Sobel et al., 2014; J.-Y. Yu et al., 1998). Using observations from Tropical Atmosphere Ocean (TAO) buoys and the SeaWinds scatterometer on the NASA Quick Scatterometer (QuikSCAT) satellite during the boreal winter in the west Pacific Ocean, Araligidad and Maloney (2008) reported a similar importance of surface flux anomalies for maintenance of deep MJO convection there.

Although the MJO is most pronounced over the eastern Indian Ocean and western Pacific during the boreal winter, during boreal summer the MJO perturbs convection north of the equator in the tropical east Pacific (e.g., Maloney et al., 2008), where similar coherence of surface heat flux and precipitation perturbations are found. In particular, Maloney and Esbensen (2003) showed a strong relationship between convection and latent heat flux anomalies during intraseasonal oscillation events, with periods of low-level westerly anomalies associated with enhanced precipitation and surface fluxes in the northeast Pacific warm pool. A follow-up study using QuikSCAT wind speed and Tropical Rainfall Measuring Mission (TRMM) precipitation observations in conjunction with buoy latent heat flux also suggested the importance of wind-surface flux feedbacks to intraseasonal convection there (Maloney & Esbensen, 2007).

We note that most of the above studies about the importance of air-sea interactions to the dynamics of MJO are based on theoretical models (Emanuel, 1987; Neelin et al., 1987), global climate models (Klingaman & Woolnough, 2014; Maloney & Sobel, 2004; Sobel et al., 2008), sparse observations (Araligidad & Maloney, 2008; Grodsky et al., 2009; Riley Dellaripa & Maloney, 2015), and/or reanalysis data (Gao et al., 2016). Further, the QuikSCAT fields used in some of the studies are limited by attenuation of surface wind speed retrievals in raining regions. In general, these results suggest the importance of wind-induced surface flux feedbacks to MJO convection. However, the importance of wind-induced surface flux anomalies to the MJO has not been examined in a global satellite data set with strong capability in raining regions like that provided by the global positioning system (GPS) radio occultation technique to retrieve the wind speed and associated surface latent heat fluxes. This motivates our current study.

In the present study, wind-induced surface flux feedbacks and their effect on the MJO are investigated in the Cyclone Global Navigation Satellite System (CYGNSS; Ruf et al., 2016) data set and an associated latent heat flux data set derived from this (Crespo et al., 2019). CYGNSS is a relatively new tool (i.e., launched in December 2016) that can be utilized to address outstanding MJO questions related to surface feedbacks as it can provide better spatial and temporal resolution of surface wind speed over the tropical oceans than other satellite retrieval platforms. With a combination of eight microsatellites that receive direct and scattered GPS signals from the ocean surface, CYGNSS provides ocean surface wind speed retrievals that are not affected by precipitation to the same degree as space borne scatterometer-based measurements that use backscattered microwave radar pulses.

The outline of this study is as follows. First, the intraseasonal surface flux-precipitation relationship will be examined in CYGNSS and compared to that derived from previous studies using buoy data. It will be shown that enhanced MJO precipitation in the Indo-Pacific warm pool during boreal winter is associated with enhanced CYGNSS wind speeds and surface latent heat fluxes that help support MJO moisture and MSE anomalies. The relative amplitude of the surface flux anomalies will be compared to that of column longwave radiative flux perturbations in the context of the MSE budget. We will then show that wind-induced surface fluxes also help support the MJO over the eastern Pacific warm pool during boreal summer, consistent with previous studies. Conclusions then follow.

2. Data and Methodology

2.1. Data

We examine the impacts of wind-induced surface flux on the MJO using CYGNSS satellite observations from 18 March 2017 to 31 December 2019 (Ruf et al., 2016). To assess the sensitivity of results to CYGNSS generation, we examined the two most recent CYGNSS wind speed products. These include Level 2 retrievals from science data record version 2.1 and climate data record (CDR) version 1.0 surface wind speed products. The CDR product uses trackwise corrections that remove biases due to uncertain GPS transmitter power and other factors. The CYGNSS wind speed products used here are estimated assuming that the sea state is in equilibrium with the wind speed, or "fully developed seas," which is the preferred product to be used over most of the tropics away from tropical cyclones (Clarizia et al., 2018). We also use the Level 2 surface latent heat flux product derived from CYGNSS wind speed coupled with thermodynamic variables from reanalysis data, as described by Crespo et al. (2019). This surface flux product was generated from CYGNSS version 2.1 wind speed, and a flux product is not available for CDR version 1.0. Both wind speed and latent heat flux were first regridded to a $1° \times 1°$ latitude-longitude grid and daily temporal resolution using the technique proposed by Ruf (2018). We also compared the CYGNSS wind speed and surface fluxes to respective fields from the OAFlux product (L. Yu & Weller, 2007), which generally showed consistent results (not shown).

Daily precipitation from the Integrated Multi-satellitE Retrievals for Global Precipitation Measurement (GPM IMERG) version 6 product averaged onto a 1° grid (Huffman et al., 2015) is used to represent intraseasonal precipitation variability to compare to CYGNSS-derived wind speed and fluxes. The period analyzed encompasses that of the CYGNSS data record.

Finally, we also employed daily 850-hPa zonal winds from the fifth global reanalysis produced by the European Center for Medium-Range Weather Forecasts (ERA5; Hersbach et al., 2020) and interpolated daily OLR from the National Oceanic and Atmospheric Administration (NOAA) polar-orbiting satellite product (Liebmann & Smith, 1996), both first regridded onto a $2.5° \times 2.5°$ grid to construct the combined empirical orthogonal function (EOF) analysis used as a compositing basis for east Pacific intraseasonal variability (discussed below). The OLR product was also used to determine the magnitude of column-integrated longwave radiation perturbations relative to intraseasonal precipitation for comparison to the CYGNSS-derived flux results.

2.2. Methods

To examine air-sea interactions associated with the MJO, all data were first band-pass filtered to 30–90 days to retain timescales characteristic of the MJO, except in the coherence analysis. We focus on the boreal winter (November to April) and boreal summer (May to October) separately given the different nature of intraseasonal variability during these two periods. The local correlations of band-pass filtered CYGNSS wind speed and latent heat flux with GPM precipitation (see Figure S1 in the supporting information) indicate high correlations over the Indian Ocean and western Pacific during the boreal winter, generally in regions where MJO amplitude is strong (e.g., Wheeler & Hendon, 2004). Another region of high correlation occurs over the eastern north Pacific during the boreal summer. In general, all of these regions have been argued in the past using buoys and other measurements to be regions of strong coupling between wind-driven surface fluxes and MJO precipitation (Araligidad & Maloney, 2008; Maloney & Esbensen, 2007; Riley Dellaripa & Maloney, 2015). However, differences in the relative importance of wind-driven surface fluxes to the overall MSE budget might be expected among these regions given different SST and zonal wind states, different convective heights between the east Pacific and Indo-Pacific warm pool, and thus different strength vertical MSE advection and cloud feedbacks, and a greater importance for horizontal advection in closing the east Pacific MSE budget, among other factors (e.g., Back & Bretherton, 2006; Maloney et al., 2014; Peters et al., 2008). Thus, in a portion of the paper, we will focus on the three sectors of the tropical ocean including the Indian ocean (10–0°S, 80–100°E), West Pacific (10–0°S, 160–180°E), and East Pacific (5–15°N, 90–110°W), which are also regions of strong convective coupling and MJO activity (see Figures S1 and S3). Results at specific grid boxes within these regions are also presented in the supporting information to allow direct comparison to previous buoy studies. In addition to more general statistical comparisons, we also conduct MJO phase composites using the global real-time multivariate MJO (RMM) index (Wheeler & Hendon, 2004, which can be downloaded at http://www.bom.gov.au/climate/mjo/) to verify that intraseasonal variability during the CYGNSS period looks like the MJO and to reinforce the regions of prominent

precipitation and surface flux variability. The composite MJO anomaly fields for each phase are constructed from days when the RMM amplitude is greater than 0.5.

To highlight boreal summer MJO variability in the east Pacific, a local eastern Pacific MJO index is also generated from the first principal component (PC1) of the leading combined EOF of 30–90 filtered ERA5 850 hPa zonal wind and NOAA OLR over the eastern north Pacific domain (0–30°N, 75–125°W) that explains about 24.5% of the total variance. Rydbeck et al. (2013) showed in a modeling study that intraseasonal events in the east Pacific can occur independent of MJO activity in the Eastern Hemisphere, but that the two tend to phase lock. The method used is similar to that employed in Maloney and Hartmann (2001), except that a combined EOF analysis is done rather than using a single 850-hPa zonal wind field to construct the index. To ensure the robustness of the EOF pattern, we derived the leading EOF and PC using 20 years of data (2000–2019). Days with the PC greater than 0.5 standard deviation during the CYGNSS period (i.e., 18 March 2017 to 31 December 2019, which includes 11 events) were used for the composite analysis. Following Maloney and Esbensen (2007), we also removed any residual climatological seasonal cycle of the filtered fields before compositing MJO anomalies to isolate the portion of the variability unrelated to climatological intraseasonal oscillations like the midsummer drought (e.g., Magaña et al., 1999).

3. Results

3.1. Boreal Winter Over the Indian Ocean and Western Pacific

As our goal here is to understand wind-induced surface flux and its role in supporting MJO convection, we first generate scatterplots of the boreal winter 30- to 90-day filtered CYGNSS wind speed versus GPM precipitation anomalies averaged over the Indian ocean and western Pacific domains (Figures 1a and 1b). Correlation coefficients between wind speed and precipitation anomalies are 0.7 over Indian ocean and about 0.8 over the western Pacific, indicating that periods of enhanced intraseasonal precipitation are associated with enhanced wind speeds. We also note a consistency across the different generations of CYGNSS products, although the version 2.1 wind speed regression coefficient with precipitation is slightly stronger than with CDR version 1.0 because some high wind speed values have been removed in CDR version 1.0 (Ruf & Twigg, 2020). Increased wind speed can enhance the surface latent heat flux, thus supporting MJO convection through moistening, as examined below.

In the context of MSE budget, the buoy results of Araligidad and Maloney (2008) and Riley Dellaripa and Maloney (2015) showed that intraseasonal latent heat flux anomalies are predominantly wind-driven and 7–10% of precipitation anomalies, which is important in the context of the column MSE budget but smaller than the contribution from radiation (~17% including all spatial scales) as examined by Adames and Kim (2016). Comparable CYGNSS results with scatterplots of MJO latent heat flux and precipitation over the Indian Ocean and western Pacific are shown in Figures 1c and 1d. Note that precipitation is in energy units (W m^{-2}, which divided by ρL and multiplied by 8.64×10^4 s day^{-1} becomes mm day^{-1}, where ρ is the density of liquid water, i.e., 1 kg m^{-2} mm^{-1}, and L is latent heat of condensation). Regression coefficients between latent heat flux and precipitation indicate that latent heat flux anomalies are about 9% of the precipitation anomalies over the Indian ocean with a correlation of 0.75. Previous work suggests that more than 90% of these anomalous fluxes are wind induced (see Figure 6 in Riley Dellaripa & Maloney, 2015). The magnitude of latent heat flux anomalies relative to precipitation is slightly smaller over the western Pacific (about 7%). These results support previous studies that indicate a strong relationship between intraseasonal latent heat flux and precipitation. We note that the relative ratio of OLR anomalies (a measure of column longwave radiative heating anomalies) to precipitation anomalies, 16% and 12% over the Indian ocean and western Pacific, respectively (Figures 1e and 1f), is larger than that of latent heat flux anomalies, consistent with previous studies. The magnitude of intraseasonal OLR anomalies relative to precipitation may be smaller than in Adames and Kim (2016) because our values are computed over a more limited time period.

To further quantify the relationship between latent heat flux and precipitation, we examine the coherence and phase relationship between the two fields (Figure 2). There is a broad peak in coherence on the 30- to 90-day MJO timescale between latent heat flux and precipitation with maximum coherence squared over 0.7 (and is above the 95% statistically significant level, which was calculated based on Thompson, 1979) over both Indian and western Pacific Oceans (Figures 2a and 2c). In both the west Pacific and Indian Oceans, precipitation and latent heat flux anomalies on MJO timescales are nearly in phase, with precipitation leading

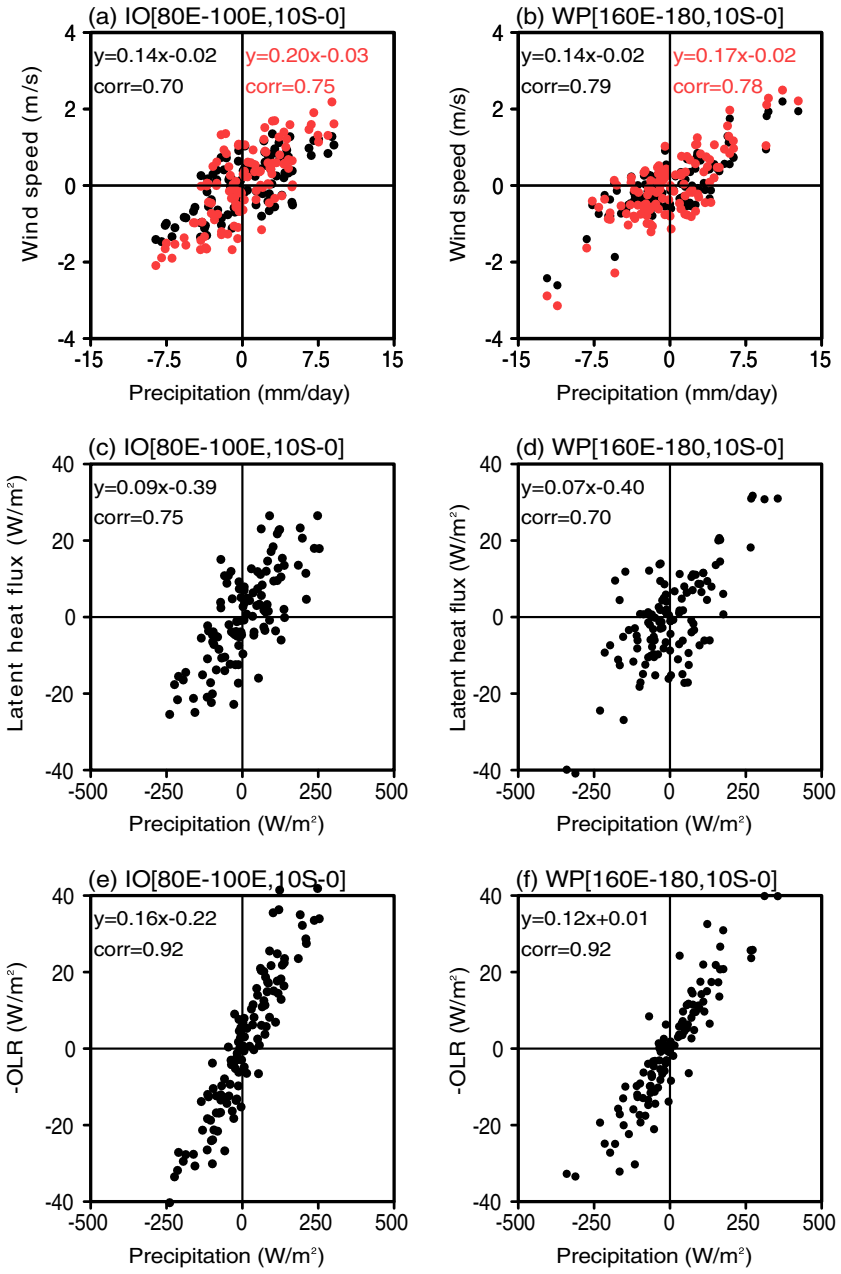

Figure 1. Scatterplots of boreal winter (November–April) 30- to 90-day band-pass filtered CYGNSS wind speed and GPM precipitation anomalies averaged over the (a) Indian ocean (IO; 80–100°E, 10°S–0) and (b) West Pacific (WP; 160°E–180, 10°S–0). Dots represent 1 day of the data, with every fifth plotted. Red dots represent version 2.1, and black CDR version 1.0. (c, d) As in (a, b) but for anomalous surface latent heat flux and precipitation. (e, f) As in (c, d) but for anomalous outgoing longwave radiation (OLR) and precipitation.

latent heat flux in some instances, especially in the Indian Ocean, consistent with the lag correlation shown in Figures S2a and S2b, again emphasizing the importance of wind-induced flux anomalies for maintaining MJO convection. The phase relationships shown here are also similar to those derived from buoy results in Riley Dellaripa and Maloney (2015). MJO composites based on the RMM index (Figure S3) indicate similar relative magnitude and phase relationship between surface flux anomalies and precipitation anomalies as in the more general analysis shown in Figures 1 and 2. These composites also resemble those found in previous MJO studies for boreal winter in the Indian and west Pacific Oceans (e.g., Waliser et al., 2009).

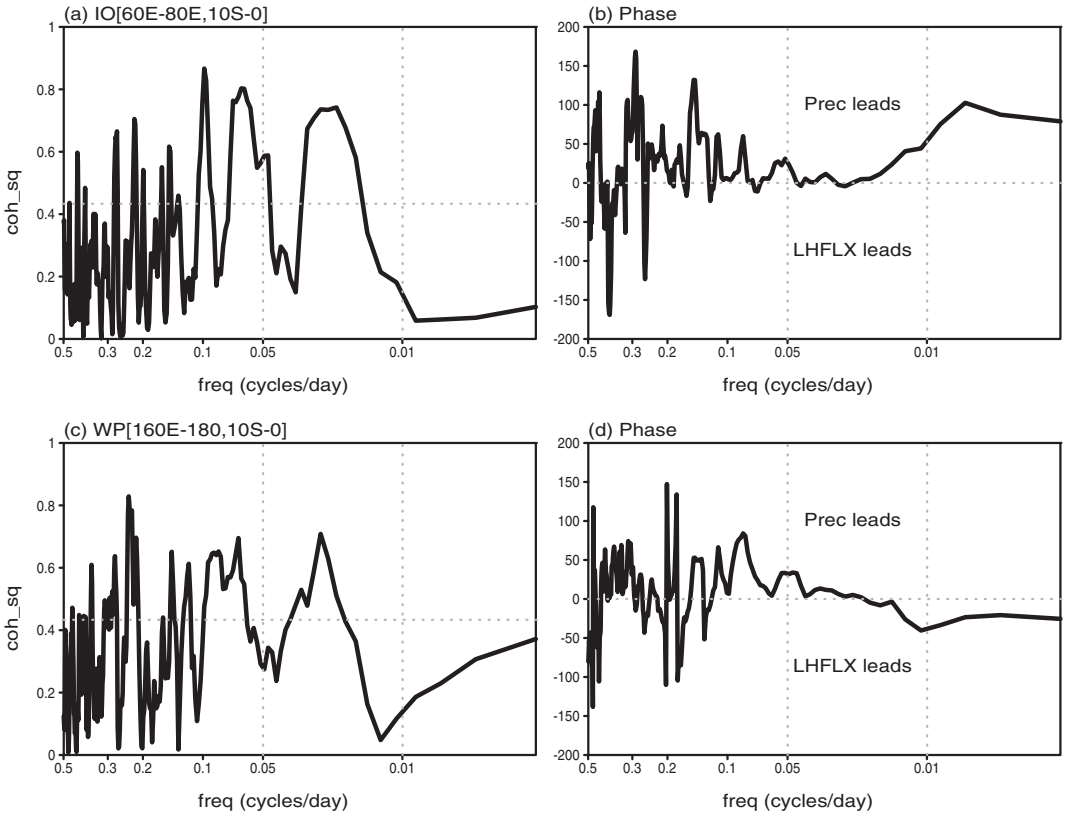

Figure 2. Coherence squared and phase between latent heat flux (LHFLX) and precipitation over the (a, b) Indian ocean (IO; 80–100°E, 10°S–0) and (c, d) West Pacific (WP; 160°E–180, 10°S–0). The horizontal dotted lines in (a) and (c) represent the 95% significance level, while the vertical dotted lines bracket the MJO timescale of 20–100 days.

In general, Figures 1–2 show that the CYGNSS wind speed and latent heat flux relationship with precipitation is similar to that produced in previous buoys studies, and that wind-induced flux feedbacks may be important for maintaining MJO convection. To directly confirm this, we provide CYGNSS results at the same locations as some of the previous buoy studies (see Figures S4 and S5 in the supporting information): (i) Over the western Pacific at 5°S, 165°E, the CYGNSS latent heat flux anomaly is approximately 10% of the precipitation anomaly. While this value is about half of that calculated from the TAO buoy analysis of Araligidad and Maloney (2008), in that study latent heat flux was calculated as an independent variable and so results are not directly comparable to the result shown here. (ii) Over the Indian Ocean at 0°, 90°E, our CYGNSS latent heat flux anomaly is about 8% of precipitation anomaly, consistent with the RAMA buoy results reported by Riley Dellaripa and Maloney (2015). Coherence analyses over these locations were also examined (Figure S5), supporting results from the larger domain.

3.2. Boreal Summer Over the Eastern Pacific

To characterize the intraseasonal surface flux-precipitation relationship during boreal summer over the eastern Pacific, we first generate scatterplots of 30- to 90-day CYGNSS wind speed, latent heat flux, and NOAA OLR anomalies versus GPM precipitation anomalies during May–October averaged over the eastern Pacific domain (Figures 3a–3c). The average correlation coefficient between MJO precipitation and wind speed is about 0.6 for the two retrievals used, and between MJO precipitation and latent heat flux is 0.63. These results support previous observations derived from buoys as well as NCEP-NCAR reanalysis (Maloney & Esbensen, 2003), which indicate a strong relationship exists between summer time wind-induced latent heat flux variations and intraseasonal precipitation over the east Pacific warm pool. The slope of the regression line in Figure 3b implies that latent heat flux anomalies are about 12% of precipitation anomalies, which is slightly larger than the values in the Indian ocean and west Pacific (c.f., Figures 1c and 1d). Interestingly, the contribution of OLR anomalies to precipitation anomalies are only 9%, which is smaller

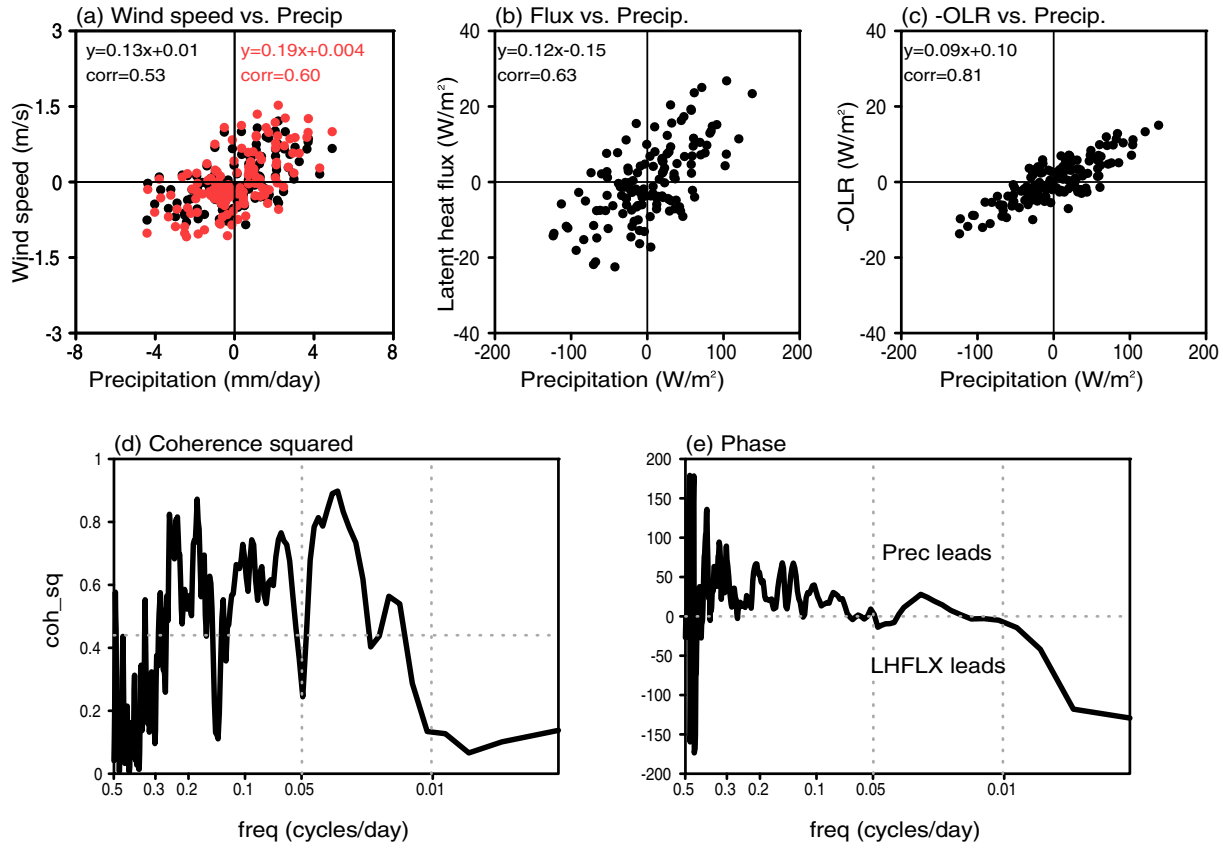

Figure 3. Same as Figures 1 and 2, but for boreal summer (May–October) averaged over the eastern north Pacific (90–110°W, 5–15°N). (a) scatterplot of wind speed and precipitation, (b) scatterplot of surface latent heat flux and precipitation, (c) scatterplot of -OLR and precipitation, (d) coherence squared and (e) phase relationship between latent heat flux (LHFLX) and precipitation.

than the contribution from latent heat fluxes, implying that latent heat flux anomalies are dominant for maintaining the MJO in the east Pacific. Convective heights in the east Pacific are generally lower than the west Pacific, which might explain the lower OLR anomalies per unit precipitation (e.g., Yokoyama & Takayabu, 2012). Similar to Figure 2, a coherence squared plot between precipitation and latent heat flux over the eastern north Pacific shows high coherence in the intraseasonal band with precipitation and latent heat flux largely in phase with each other, though occasionally precipitation leads latent heat flux (Figures 3d and 3e).

Composite patterns of 850-hPa zonal wind and OLR together with CYGNSS wind speed, latent heat flux, and GPM precipitation anomalies associated with the leading combined EOF (see Figure S6 in the supporting information for the EOF1 pattern) are shown in Figure 4, defined using positive events in the index. Consistent with Maloney and Esbensen (2003, 2005, 2007), positive events in EOF1 are associated with low-level westerly winds and enhanced convection that peaks north of 10°N (Figures 4a and 4b). Variability in this region also coincides with the eastern Pacific hurricane genesis region (Maloney & Hartmann, 2000). Although low-level zonal wind anomalies extend westward across the Pacific, the intensification of surface wind speed is mainly confined to the east of 110°W, consistent with the results from MJO events in Maloney and Esbensen (2003, 2007). Unlike for QuikSCAT wind speed anomalies (see Figure 5 in Maloney & Esbensen, 2007) that tend to be centered in a band between about 8 and 10°N that extends to 120°W, CYGNSS wind speed anomalies fields are more confined near the coasts of Mexico and Central America. This may be due to the fact that QuikSCAT cannot detect wind speed in rainy conditions. Therefore, our analysis highlights one potential advantage of using CYGNSS instead of scatterometer fields. We also note consistency in the wind speed anomaly patterns for the two CYGNSS versions, although version 2.1 shows a larger magnitude than CDR version 1.0 (Figures 4c and 4d).

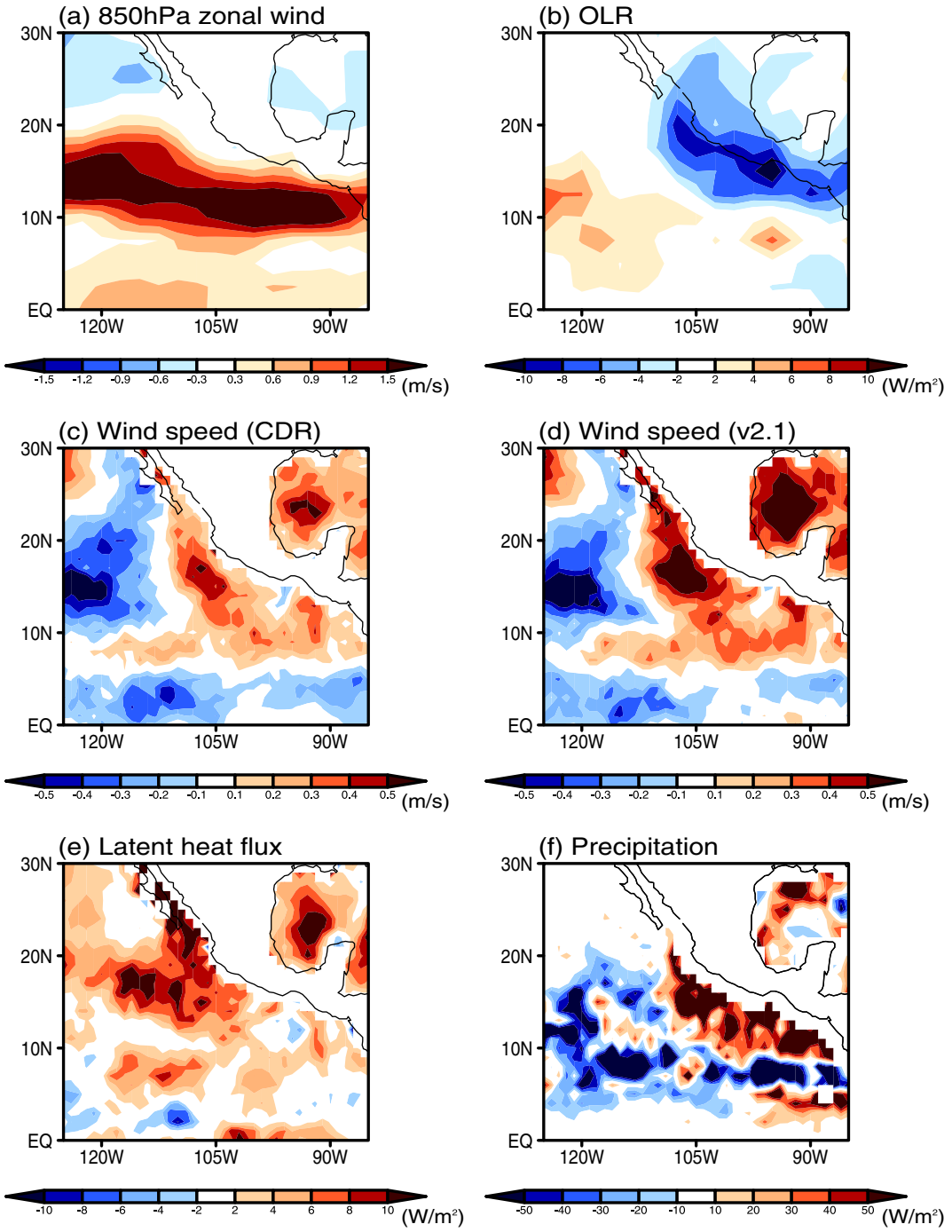

Figure 4. Composite anomalies based on the east Pacific PC1 timeseries for (a) ERA5 850 hPa zonal wind, (b) NOAA outgoing longwave radiation (OLR), (c) CYGNSS wind speed (CDR version 1.0), (d) CYGNSS wind speed (version 2.1), (e) CYGNSS latent heat flux, and (f) GPM precipitation over the eastern north Pacific during boreal summer (May–October).

Higher wind speed regions tend to be associated with stronger MJO precipitation, although less similarity exists south of 10°N (c.f., Figures 4c, 4d, and 4f). In addition, positive MJO wind speed anomalies in the eastern part of the domain are accompanied by positive latent heat flux anomalies (c.f., Figures 4c, 4d, and 4e). There, the surface latent heat flux anomaly field shows similar behavior to that of wind speed with large values near 15°N, 110°W in the east Pacific and in the Gulf of Mexico where positive wind speed anomalies

occur. Poorer agreement occurs west of 110°W, suggesting that thermodynamic factors may play a larger role in regulating latent heat flux in that region. This behavior is different than that shown in the reanalysis fields of Maloney and Esbensen (2003) where the pattern of latent heat flux anomalies more strongly matched that of wind speed, a difference that might be caused by the limited 3-year period analyzed here. Regardless, latent heat flux anomalies are generally supportive of the MJO-related precipitation anomalies in this region, especially near the coasts of Mexico and Central America, consistent with previous results (e.g., Maloney & Esbensen, 2003). These results suggest that wind-induced surface fluxes may help to support boreal summer MJO convection over the east Pacific, consistent with the previous modeling experiments of Maloney and Esbensen (2005) and buoys study of Maloney and Esbensen (2007).

4. Concluding Remarks

Gridded daily wind speed and latent heat flux derived from the GPS radio occultation retrievals of the CYGNSS satellite from 18 March 2017 to 31 December 2019 were analyzed to assess the importance of wind-induced surface flux anomalies to MJO convection. Besides providing a better spatial and temporal resolution, CYGNSS wind speed retrievals are not as negatively affected by precipitation compared to other space-based measurements, thus providing useful information about the role of surface fluxes for the maintenance of MJO convection. Our analyses show consistent results between the two versions of CYGNSS wind speed (i.e., the science data record version 2.1 and the CDR version 1.0), although the version 2.1 demonstrates higher amplitude anomalies than in the CDR. Our main results are summarized as follows:

1. Intraseasonal precipitation anomalies over the Indo-Pacific warm pool during boreal winter and the eastern north Pacific warm pool during boreal summer are associated with enhanced wind speed and surface latent heat fluxes that help support convection. As shown in Figures 1 and 3 (and Figures S4 in the supporting information), surface latent heat flux anomalies contribute to around 7–12% of intraseasonal precipitation anomalies, compared to about 9–16% from OLR anomalies. These values are consistent with previous studies from buoy data (e.g., Araligidad & Maloney, 2008; Riley Dellaripa & Maloney, 2015), and suggest that surface flux anomalies are important for maintenance of MJO convection.
2. Coherence analysis of precipitation and latent heat flux show high coherence at the intraseasonal timescale and a similar phase relationship between precipitation and latent heat flux in the three regions examined, with precipitation general in phase with, but occasionally leading latent heat flux (Figures 2 and 3).
3. The composite pattern of intraseasonal wind speed, latent heat flux, and precipitation anomalies over the eastern north Pacific during boreal summer events supports the idea that wind-induced latent heat flux anomalies help sustain MJO convection there (Figure 4).

Our results highlight the usefulness of the CYGNSS data set for investigations of the MJO and support findings from previous studies on the MJO-surface flux relationship. With increased coverage and the ability to measure in regions of heavy rainfall, this data set provides insights on the MJO that do not rely on the assumptions inherent in reanalysis data. Since the current results are based on less than 3 years of CYGNSS data, it is critical to reexamine the robustness of the results derived here as a longer CYGNSS data record becomes available with new versions of CYGNSS products as algorithmic improvements continue to be made. Regardless, a robust conclusion of our current study is that wind-induced surface fluxes are important for supporting MJO convection.

Data Availability Statement

We thank the NASA CYGNSS science and operations teams for providing the data, which can be downloaded at https://podaac.jpl.nasa.gov/CYGNSS, and to Juan Crespo, Derek Posselt, and Shakeel Asharaf for generating the CYGNSS surface flux data. The ERA5 horizontal wind and NOAA outgoing longwave radiation data are obtained from the NCAR Research Data Archive (https://doi.org/10.5065/BH6N-5N20) and NOAA Physical Sciences Laboratory (https://psl.noaa.gov/data/gridded/data.interp_OLR.html), respectively. We also thank the NASA Goddard Space Flight Center for providing the global precipitation measurement (GPM) precipitation (https://gpm.nasa.gov/data-access/downloads/gpm) and the WHOI OAFlux project for providing the global ocean heat flux and wind speed products (http://oaflux.whoi.edu/data.html).

Acknowledgments
This work was supported by NASA CYGNSS grant NNX17AH77G and NOAA CVP grant NA18OAR4310299.

References

Adames, Á. F., & Kim, D. (2016). The MJO as a dispersive, convectively coupled moisture wave: Theory and observations. *Journal of the Atmospheric Sciences*, *73*(3), 913–941. https://doi.org/10.1175/JAS-D-15-0170.1

Andersen, J. A., & Kuang, Z. (2012). Moist static energy budget of MJO-like disturbances in the atmosphere of a zonally symmetric aquaplanet. *Journal of Climate*, *25*(8), 2782–2804. https://doi.org/10.1175/jcli-d-11-00168.1

Araligidad, N. M., & Maloney, E. D. (2008). Wind-driven latent heat flux and the intraseasonal oscillation. *Geophysical Research Letters*, *35*, L04815. https://doi.org/10.1029/2007GL032746

Back, L. E., & Bretherton, C. S. (2005). The relationship between wind speed and precipitation in the Pacific ITCZ. *Journal of Climate*, *18*(20), 4317–4328. https://doi.org/10.1175/JCLI3519.1

Back, L. E., & Bretherton, C. S. (2006). Geographic variability in the export of moist static energy and vertical motion profiles in the tropical Pacific. *Geophysical Research Letters*, *33*, L17810. https://doi.org/10.1029/2006GL026672

Clarizia, M. P., Zavorotny, V. & Ruf, C. (2018). Level 2 wind speed retrieval. Algorithm theoretical basis document. *CYGNSS project document*, 148-0138, Rev 5, 17 Aug. 2018.

Crespo, J., Posselt, D., & Asharaf, S. (2019). CYGNSS surface heat flux product development. *Remote Sensing*, *11*(19), 2294. https://doi.org/10.3390/rs11192294

DeMott, C. A., Klingaman, N. P., & Woolnough, S. J. (2015). Atmosphere-ocean coupled processes in the Madden-Julian oscillation. *Reviews of Geophysics*, *53*, 1099–1154. https://doi.org/10.1002/2014RG000478

Emanuel, K. A. (1987). An air-sea interaction model of intraseasonal oscillations in the tropics. *Journal of the Atmospheric Sciences*, *44*(16), 2324–2340. https://doi.org/10.1175/1520-0469(1987)044<2324:AASIMO>2.0.CO;2

Gao, Y., Hsu, P.-C., & Hsu, H.-H. (2016). Assessments of surface latent heat flux associated with the Madden-Julian oscillation in reanalyses. *Climate Dynamics*, *47*(5-6), 1755–1774. https://doi.org/10.1007/s00382-015-2931-4

Grodsky, S. A., Bentamy, A., Carton, J. A., & Pinker, R. T. (2009). Intraseasonal latent heat flux based on satellite observations. *Journal of Climate*, *22*(17), 4539–4556. https://doi.org/10.1175/2009JCLI2901.1

Hersbach, H., Bell, B., Berrisford, P., Hirahara, S., Horányi, A., Muñoz-Sabater, J., et al. (2020). The ERA5 global reanalysis. *Quarterly Journal of the Royal Meteorological Society*, *146*(730), 1999–2049. https://doi.org/10.1002/qj.3803

Huffman, G. J., Bolvin, D. T., Braithwaite, D., Hsu, K., Joyce, R., Xie, P., & Yoo, S. H. (2015). NASA global precipitation measurement (GPM) integrated multi-satellite retrievals for GPM (IMERG). *Algorithm Theoretical Basis Document (ATBD)*, 1-26, Version 4.5, 16 November 2015.

Klingaman, N. P., & Woolnough, S. J. (2014). The role of air-sea coupling in the simulation of the Madden-Julian oscillation in the Hadley Centre model. *Quarterly Journal of the Royal Meteorological Society*, *140*(684), 2272–2286. https://doi.org/10.1002/qj.2295

Liebmann, B., & Smith, C. A. (1996). Description of a complete (interpolated) outgoing longwave radiation dataset. *Bulletin of the American Meteorological Society*, *77*, 1275–1277. www.jstor.org/stable/26233278

Madden, R. A., & Julian, P. R. (1971). Detection of a 40–50 day oscillation in the zonal wind in the tropical Pacific. *Journal of the Atmospheric Sciences*, *28*(5), 702–708. https://doi.org/10.1175/1520-0469(1971)028<0702:DOADOI>2.0.CO;2

Madden, R. A., & Julian, P. R. (1972). Description of global-scale circulation cells in the tropics with a 40–50 day period. *Journal of the Atmospheric Sciences*, *29*(6), 1109–1123. https://doi.org/10.1175/1520-0469(1972)029<1109:DOGSCC>2.0.CO;2

Magaña, V., Amador, J. A., & Medina, S. (1999). The midsummer drought over Mexico and Central America. *Journal of Climate*, *12*(6), 1577–1588. https://doi.org/10.1175/1520-0442(1999)012<1577:TMDOMA>2.0.CO;2

Maloney, E. D. (2009). The moist static energy budget of a composite tropical intraseasonal oscillation in a climate model. *Journal of Climate*, *22*(3), 711–729. https://doi.org/10.1175/2008JCLI2542.1

Maloney, E. D., Chelton, D. B., & Esbensen, S. K. (2008). Subseasonal SST variability in the tropical eastern north Pacific during boreal summer. *Journal of Climate*, *21*(17), 4149–4167. https://doi.org/10.1175/2007JCLI1856.1

Maloney, E. D., & Esbensen, S. K. (2003). The amplification of east Pacific Madden-Julian oscillation convection and wind anomalies during June–November. *Journal of Climate*, *16*(21), 3482–3497. https://doi.org/10.1175/1520-0442(2003)016<3482:TAOEPM>2.0.CO;2

Maloney, E. D., & Esbensen, S. K. (2005). A modeling study of summertime east Pacific wind-induced ocean-atmosphere exchange in the intraseasonal oscillation. *Journal of Climate*, *18*(4), 568–584. https://doi.org/10.1175/JCLI-3280.1

Maloney, E. D., & Esbensen, S. K. (2007). Satellite and buoy observations of boreal summer intraseasonal variability in the tropical northeast Pacific. *Monthly Weather Review*, *135*(1), 3–19. https://doi.org/10.1175/MWR3271.1

Maloney, E. D., & Hartmann, D. L. (2000). Modulation of hurricane activity in the Gulf of Mexico by the Madden-Julian oscillation. *Science*, *287*(5460), 2002–2004. https://doi.org/10.1126/science.287.5460.2002

Maloney, E. D., & Hartmann, D. L. (2001). The Madden–Julian oscillation, barotropic dynamics, and north Pacific tropical cyclone formation. Part I: Observations. *Journal of the Atmospheric Sciences*, *58*, 2545–2558. https://doi.org/10.1175/1520-0469(2001)058<2545:TMJOBD>2.0.CO;2

Maloney, E. D., Jiang, X., Xie, S.-P., & Benedict, J. J. (2014). Process-oriented diagnosis of east Pacific warm pool intraseasonal variability. *Journal of Climate*, *27*(16), 6305–6324. https://doi.org/10.1175/JCLI-D-14-00053.1

Maloney, E. D., & Sobel, A. H. (2004). Surface fluxes and ocean coupling in the tropical intraseasonal oscillation. *Journal of Climate*, *17*(22), 4368–4386. https://doi.org/10.1175/JCLI-3212.1

Maloney, E. D., Sobel, A. H., & Hannah, W. M. (2010). Intraseasonal variability in an aquaplanet general circulation model. *Journal of Advances in Modeling Earth Systems*, *2*, 5. https://doi.org/10.3894/JAMES.2010.2.5

Neelin, J. D., Held, I. M., & Cook, K. H. (1987). Evaporation-wind feedback and low-frequency variability in the tropical atmosphere. *Journal of the Atmospheric Sciences*, *44*(16), 2341–2348. https://doi.org/10.1175/1520-0469(1987)044<2341:EWFALF>2.0.CO;2

Peters, M. E., Kuang, Z., & Walker, C. C. (2008). Analysis of atmospheric energy transport in ERA-40 and implications for simple models of the mean tropical circulation. *Journal of Climate*, *21*(20), 5229–5241. https://doi.org/10.1175/2008JCLI2073.1

Riley Dellaripa, E. M., & Maloney, E. D. (2015). Analysis of MJO wind-flux feedbacks in the Indian ocean using RAMA buoy observations. *Journal of the Meteorological Society of Japan Series II*, *93A*(0), 1–20. https://doi.org/10.2151/jmsj.2015-021

Ruf, C. S. (2018). Algorithm theoretical basis document. Level 3 gridded wind speed. *CYGNSS project document*, 148-0319, Rev 1, 20 Aug. 2018.

Ruf, C. S., Atlas, R., Chang, P. S., Clarizia, M. P., Garrison, J. L., Gleason, S., et al. (2016). New ocean winds satellite mission to probe hurricanes and tropical convection. *Bulletin of the American Meteorological Society*, *97*(3), 385–395. https://doi.org/10.1175/BAMS-D-14-00218.1

Ruf, C. S. & Twigg, D. (2020). Algorithm theoretical basis document. Level 1 & 2 trackwise corrected climate data record. *CYGNSS project document*, 148-0389, Rev 0, 26 Mar. 2020.
Rydbeck, A. V., Maloney, E. D., Xie, S.-P., Hafner, J., & Shaman, J. (2013). Remote forcing versus local feedback of east Pacific intraseasonal variability. *Journal of Climate*, *26*(11), 3575–3596. https://doi.org/10.1175/JCLI-D-12-00499.1
Shinoda, T., Hendon, H. H., & Glick, J. (1998). Intraseasonal variability of surface fluxes and sea surface temperature in the tropical western Pacific and Indian oceans. *Journal of Climate*, *11*(7), 1685–1702. https://doi.org/10.1175/1520-0442(1998)011<1685:IVOSFA>2.0.CO;2
Sobel, A., Wang, S., & Kim, D. (2014). Moist static energy budget of the MJO during DYNAMO. *Journal of the Atmospheric Sciences*, *71*(11), 4276–4291. https://doi.org/10.1175/JAS-D-14-0052.1
Sobel, A. H., Maloney, E. D., Bellon, G., & Frierson, D. M. (2008). The role of surface heat fluxes in tropical intraseasonal oscillations. *Nature Geoscience*, *1*(10), 653–657. https://doi.org/10.1038/ngeo312
Sobel, A. H., Maloney, E. D., Bellon, G., & Frierson, D. M. (2010). Surface fluxes and tropical intraseasonal variability: A reassessment. *Journal of Advances in Modeling Earth Systems*, *2*, 27. https://doi.org/10.3894/JAMES.2010.2.2
Thompson, R. O. R. Y. (1979). Coherence significance levels. *Journal of the Atmospheric Sciences*, *36*(10), 2020–2021. https://doi.org/10.1175/1520-0469(1979)036<2020:CSL>2.0.CO;2
Waliser, D. E., Sperber, K., Hendon, H., Kim, D., Maloney, E., & Wheeler, M. (2009). MJO simulation diagnostics. *Journal of Climate*, *22*(11), 3006–3030. https://doi.org/10.1175/2008JCLI2731.1
Wheeler, M. C., & Hendon, H. H. (2004). An all-season real-time multivariate MJO index: Development of an index for monitoring and prediction. *Monthly Weather Review*, *132*(8), 1917–1932. https://doi.org/10.1175/1520-0493(2004)132<1917:AARMMI>2.0.CO;2
Wolding, B. O., & Maloney, E. D. (2015). Objective diagnostics and the Madden-Julian Oscillation. Part II: Application to moist static energy and moisture budgets. *Journal of Climate*, *28*, 7786–7808.
Yokoyama, C., & Takayabu, Y. N. (2012). Relationships between rain characteristics and environment. Part I: TRMM precipitation features and the large-scale environment over the tropical Pacific. *Monthly Weather Review*, *140*(9), 2831–2840. https://doi.org/10.1175/MWR-D-11-00252.1
Yu, J.-Y., Chou, C., & Neelin, J. D. (1998). Estimating the gross moist stability of the tropical atmosphere. *Journal of the Atmospheric Sciences*, *55*(8), 1354–1372. https://doi.org/10.1175/1520-0469(1998)055<1354:ETGMSO>2.0.CO;2
Yu, L., & Weller, R. A. (2007). Objectively analyzed air–sea heat fluxes for the global ice-free oceans (1981–2005). *Bulletin of the American Meteorological Society*, *88*(4), 527–540. https://doi.org/10.1175/BAMS-88-4-527
Zhang, C. (2005). Madden-Julian oscillation. *Reviews of Geophysics*, *43*, RG2003. https://doi.org/10.1029/2004RG000158
Zhang, C. (2013). Madden–Julian oscillation: Bridging weather and climate. *Bulletin of the American Meteorological Society*, *94*(12), 1849–1870. https://doi.org/10.1175/BAMS-D-12-00026.1
Zhang, C., & McPhaden, M. J. (2000). Intraseasonal surface cooling in the equatorial western Pacific. *Journal of Climate*, *13*(13), 2261–2276. https://doi.org/10.1175/1520-0442(2000)013<2261:ISCITE>2.0.CO;2